Environmental Science Advances

ROYAL SOCIETY OF CHEMISTRY

PAPER

View Article Online
View Journal | View Issue

Cite this: *Environ. Sci.: Adv.*, 2024, **3**, 436

Role of extracellular polymeric substances in selenite and tellurite reduction by waste activated and anaerobic sludge†

Sudeshna Saikia, *[a] Kannan Pakshirajan[b] and Piet N. L. Lens[a]

This study investigated the role of Extracellular Polymeric Substances (EPS) extracted from waste activated sludge (WAS) and anaerobic granular sludge (AGS) on the reduction of selenite and tellurite. The tightly bound fraction of EPS (TB-EPS) from AGS gave the highest (>95%) removal efficiency of selenite and tellurite. The EPS reduced these oxyanions to their elemental forms as either selenium (Se) or tellurium (Te) nanoparticles (NPs) in mono metalloid incubations as well as conjugated (Se–Te) NPs for bi-metalloid incubations. The NPs were treated with two detergents and two enzymes to remove portions of the EPS coating of the NPs. The capping material was quantified along with the measurement of parameters such as size, surface charge and polydispersity. The smaller size (24.7–123 nm) and higher negative zeta-potential (−33.5 mV) of Se–Te NPs in conjugated form indicates more structural integrity compared to the Se and Te NPs in their individual form. The intermolecular interactions of proteins and extracellular DNA (eDNA) provided enhanced colloidal stability. This work revealed the previously unexplored roles of EPS in selenite and tellurite reduction and the features of the respective NPs in individual and conjugated form.

Received 24th September 2023
Accepted 10th January 2024

DOI: 10.1039/d3va00298e

rsc.li/esadvances

Environmental significance

This study revealed the previously unrecognized role of Extracellular Polymeric Substances (EPS) in reductive detoxification of hazardous selenite and tellurite from wastewater. The resultant selenium–tellurium nanoparticles (NPs) possess excellent surface properties in conjugated forms compared to their individual forms. The regulation of the key components of EPS are important for structural stability of NPs, which might open up wider applications for engineered nanomaterials in treating wastewaters.

1. Introduction

Selenium (Se) and tellurium (Te) are widespread environmental contaminants. Both chalcogens enter different habitats through either natural sources or anthropogenic activities.[1] They share several physico-chemical properties and are primarily available in four oxidation states of +6, +4, 0 and −2. The prevalent oxyanions exist as selenite and selenate (SeO_3^{2-}, SeO_4^{2-}) as well as tellurite and tellurate (TeO_3^{2-}, TeO_4^{2-}), which are soluble and toxic to humans and aquatic ecosystems at higher concentrations.[2,3] Reduction of these oxyanions can not only abate their toxicity level, but also produces non-toxic Se and Te nanoparticles (NPs) with excellent optical, photoconductive and thermoconductive properties.[4] Both NP types possess multifaceted applications in material science including steels, solar panels, glasses, rechargeable batteries, electronics and chemical industries;[5] in therapeutics as imaging, sensing, antimicrobial[6] and anticancer agents[7] as well as in the remediation of environmental contaminants as heavy metal adsorbents.[8,9]

The reduction of Se and Te oxyanions is well documented for a variety of bacterial and fungal strains, either by pure cultures or by mixed consortia.[10] The reduction mechanism can be mediated by compounds containing a thiol functional group such as glutathione, glutaredoxin and thioredoxin.[11] Additionally, some pathways include membrane bound nitrite/nitrate reductase, fumarate reductase, sulfite reductase and selenite/tellurite reductase for dissimilaritory Se/Te reduction.[12] Dissimilatory Se/Te reduction has received increased attention in which Se/Te oxyanions are used as terminal electron acceptors for growth under anaerobic conditions and form elemental NPs, thereby reducing the toxicity and bioavailability of soluble oxyanion forms.[13] Besides producing these NPs individually, a few studies have reported co-synthesis of Se–Te nanostructures by *Bacillus selenitireducens*, *Sulfurospirillum*

[a]*Department of Microbiology, Ryan Institute, University of Galway, University Road, H91 TK33, Galway, Ireland. E-mail: sudeshnasaikia@gmail.com*

[b]*Department of Biosciences and Bioengineering, Indian Institute of Technology Guwahati, Guwahati, 781039, Assam, India*

† Electronic supplementary information (ESI) available. See DOI: https://doi.org/10.1039/d3va00298e

barnesii,[14] *Ochrobactrum* sp. MPV1 (ref. 15) and *Bacillus beveridgei*.[16] Simultaneous production of different allotropic forms of Se (trigonal) and Te (hexagonal) nanostructures has also been reported in an upflow anaerobic sludge blanket reactor (UASB) treating Se and Te oxyanions containing wastewaters.[2] Besides bacterial strains, the fungus *Phanerochaete chrysosporium* has also been investigated for production of Se–Te nanospheres when grown on selenite/tellurite together.[17]

Microbial EPS are high molecular-weight biopolymers secreted by microbial cells in the extracellular matrix.[18,19] They are predominantly composed of proteins and polysaccharides with numerous functional groups, such as amino, carboxyl, hydroxyl and phosphoryl which can react with contaminants through ion exchange, complexation or precipitation.[20] In the last few decades, the adsorption properties of EPS for pollutants and the involved mechanisms have been well investigated. Recently, the reductive properties of EPS have been recognized as well, and were shown to influence the transformation as well as the detoxification of pollutants.[21,22] Biotic reduction of selenite and tellurite mediated by microorganisms is generally recognized, however, the possible role of microbial EPS in the biotic reduction of selenite and tellurite to their respective elemental nanoparticles (NPs) is not yet known.

Biologically produced NPs have quite different surface properties than their chemical counterparts due to an innate capping material of protein like substances or extracellular polymeric substances (EPS). The EPS provide negative surface charge and hence impart structural integrity to the selenium nanoparticles (SeNPs).[1,23] Very few studies have so far reported the composition of the EPS coating of TeNPs. Although some progress has been made in understanding the effect of EPS on NP formation, previous studies have been primarily based on homogeneous NPs. Hence, we lack adequate knowledge about the impact of NPs with heterogeneous composition. Tong *et al.* (2015)[24] demonstrated that the toxicity towards *Escherichia coli* and *Aeromonas hydrophila* is attenuated in combined nano-ZnO–TiO_2 form compared to their individual (ZnO and TiO_2) form. Thus, the heterogenic NP potentially undergo physico-chemical transformations, influencing their fate and toxic potential.[25] Chemically produced Se–Te NPs are reported superior in terms of magnetoresistance and electrical resistance compared to the individual NP.[26] However, very few studies have been carried out to explore the biogenic Se–Te NPs and their surface properties in conjugated form. Therefore, elucidating the interactions and cumulative features of conjugated NPs will provide a more complete picture of the ecological impacts and technical applicability of NPs.

The objective of this study was to investigate first the effect of EPS extracted from waste activated and anaerobic granular sludge on the reduction of selenite and tellurite. Secondly, the composition of the EPS and structural parameters of the resultant NPs were studied both in individual (Se/Te NPs) and conjugated (Se–TeNPs) form. Different treatments (detergents and enzymatic digestion) were carried out to further explore the composition of the coating of the Se and Te NPs. The NPs were analysed by using a zetasizer, transmission electron microscopy (TEM), Fourier-transform infrared spectroscopy (FTIR), fluorescence excitation–emission matrix spectroscopy (FEEM) to characterise their properties.

2. Materials and methods

2.1. Source of EPS

Two types of sludges, described in details by Saikia *et al.* (2022),[9] were used for the extraction of EPS. The anaerobic granular sludge (AGS) was obtained from a wastewater treatment plant at Carbery Milk Products (Cork, Ireland). The waste activated sludge (WAS) was obtained from a secondary clarifier of a municipal wastewater treatment plant at Tuam (Galway, Ireland).

2.2. Extraction of EPS

The EPS was extracted from both sludges as loosely bound EPS (LB-EPS) and tightly-bound EPS (TB-EPS) using the protocol described by Mal *et al.* (2021).[27] The LB-EPS was collected by centrifuging the sludge at 10 000*g* for 20 min at 4 °C. For extracting the TB-EPS, the pellet was resuspended in Milli-Q water and heated to 80 °C for 30 min followed by centrifugation at 10 000*g* for 20 min at 4 °C. The supernatant in each type of EPS was filtered through a 0.45 μm syringe filter (Sigma-Aldrich, Burlington, USA) and used as stock solution for reduction experiments.

2.3. Experimental setup

2.3.1. Effect of EPS on reduction. Reduction experiments were conducted in four sets including two types of EPS (LB-EPS and TB-EPS) extracted from the two different sludges (WAS and AGS). Each set was carried out in 50 mL serum bottles containing 30 mL (working volume) mixture of 100 mg carbon per L EPS and 1.0 mM selenite and tellurite individually or in combination. The bottles were kept under anaerobic conditions on a shaking incubator at 130 rpm and 30 °C. At a predetermined specific time, 1 mL was sampled from each serum bottle at an interval of 15 minutes till 1 h, followed by one sample each day. The equilibrium was achieved in 4 days, yet the experiments were conducted for 7 days to confirm the overall removal efficiency. After each sample collection, the NPs formed were separated from the suspension by centrifugation (Thermo Scientific Centrifuge, Chelmsford, USA) at 20 000*g* for 20 min. The supernatant was collected and the amount of selenite and tellurite was quantified.[28,29]

2.3.2. Treatments of EPS in NPs. Individual and conjugated Se and Te NPs were treated with two different detergents and enzymes to remove fractions of the capping material in order to assess their impact on stability associated parameters, *e.g.* size and surface charge. The collected NPs (see Section 2.3.1.) were treated with detergents as described in Bulgarini *et al.* (2020)[30] with modification. Briefly, 100 μL of 2% Triton X-100 was added as a mild detergent to the NPs and kept in a shaker (Cole Parmer, Arlington, USA) at 130 rpm and 27 °C for 20 min. For harsh treatment, 100 μL of 10% sodium dodecyl sulfate (SDS) was added and incubated at 130 rpm and 100 °C for 30 min.

Enzymatic digestion of NPs was carried out with protease and cellulase (Fisher Scientific, Dublin, Ireland) for specific removal of the protein and polysaccharide fractions, respectively, as described in Lin *et al.* (2016).[31] Proteinase K (75 mg L^{-1}) and cellulase (75 mg mL^{-1}) was added to the phosphate buffer (pH 7.4) for the NPs treatments. For proteinase K, the samples were kept at 37 °C for 12 h and the digestion was terminated by adding 3.0 mL of 5% trichloroacetic acid (TCA) to precipitate the protein for 30 min. Cellulase treatment was carried out at 55 °C for 4 h.

All the samples after treating with detergents and enzymes were centrifuged at 15 000*g* for 20 min and the protein and polysaccharide contents were quantified (see below).

2.4. Analytical methods

Total Se and Te concentrations were determined using inductively coupled plasma – optical emission spectrometry (ICP-OES 5110, Santa Clara, USA) as described by Mal *et al.* (2016).[28] The total organic carbon (TOC) was quantified using a TOC-analyzer (Shimadzu, Tokyo, Japan) after diluting the sample with Milli-Q water at 1 : 10 ratio as described by Zhang *et al.* (2007).[32] The composition of the EPS extracted from the sludges and the NPs before and after all the treatments were analysed for protein using the modified Lowry method and polysaccharide using the phenol-sulfuric acid method as described by Jain *et al.* (2015).[33] Lipids were analysed by gas chromatography as described by Neves *et al.* (2009).[34] The extraction of extracellular DNA (eDNA) present on the NPs was carried out according to the Qiagen DNeasy extraction kit protocol (QIAGEN, Hilden, Germany). The amount of DNA was quantified using a NanoDrop spectrophotometer (Thermo Fisher, Waltham, USA).

The stability associated parameters of NPs, *i.e.*, zeta potential, hydrodynamic diameter (HDD) and polydispersity index (PDI) analyses were measured using a zetasizer (Litesizer 500, Graz, Austria) as described by Bulgarini *et al.* (2020).[30] The NPs were further characterised by FTIR (Thermo Scientific Nicolet iS5 spectrometer, Madison, USA), TEM (Hitachi 7500, Tokyo, Japan) and FEEM spectra (RF-6000 Shimadzu, Tokyo, Japan) by following the methodology of Saikia *et al.* (2022).[9]

3. Results

3.1. Effect of extracellular polymeric substances (EPS) on removal of Se and Te oxyanions

Fig. 1a shows the percentage removal of selenite by the LB and TB fractions of EPS extracted from both sludges investigated, *i.e.*, WAS and AGS. After 4 days of incubation, the levels of selenite reached equilibrium with the highest removal efficiencies of 95% by TB-EPS of AGS, followed by the LB-EPS of the same sludge. Fig. 1b shows tellurite removal efficiencies by the LB and TB fraction of EPS from WAS and AGS and gave a 98% removal efficiency with the TB-EPS from AGS. The overall removal efficiency of both selenite and tellurite obtained was in the order of TB-EPS, AGS > LB-EPS, AGS > TB-EPS, WAS > LB-EPS, WAS.

Fig. 1c shows the percentage removal of selenite from a selenite–tellurite mixture by the LB and TB fraction of EPS extracted from each of the two sludges. After 2 days incubation, the levels of selenite reached equilibrium with no significant removal observed with either of the sludges investigated. About 10% removal of selenite was observed with TB-EPS from AGS. Fig. 1d shows the tellurite removal efficiencies from the selenite–tellurite mixture by the LB and TB fractions of EPS from WAS and AGS and 93% removal efficiency was found with the TB-EPS from AGS. The removal efficiency for selenite/tellurite was in the order of TB-EPS, AGS > LB-EPS, AGS > TB-EPS, WAS > LB-EPS, WAS in both cases. The resultant NPs in each condition were further observed by the alteration in colour of the solutions before and after addition of the respective oxyanions. The red and black colour confirmed the presence of elemental Se and Te NPs, respectively, whereas the blackish red colour of the co-incubation indicated the co-synthesis of Se–Te NPs (Fig. S1 in ESI†).

The constituents of LB-EPS and TB-EPS of both sludges are shown in Fig. 2. The EPS were mainly composed of proteins and polysaccharides with a very low concentration of lipids. Considering the highest efficiency observed in all the conditions of NPs formation and composition, the TB-EPS from AGS was used in the further investigations.

3.2. Effect of detergent and enzymatic treatments on EPS composition

Both detergent, *i.e.*, SDS (Se/TeNPs–S) and Triton X (Se/TeNPs–T), as well as enzyme, *i.e.*, protease (Se/TeNPs–P) and cellulase (Se/TeNPs–C), treatment led to the removal of part of the capping material observed by the change in concentration of components in the solution after each treatment. The treatments indicated the presence of lower amounts of biochemicals compared to their respective control samples (Fig. 3). The enzymatic degradation showed more promising results in terms of removing EPS components (Fig. 3). The cellulase treated samples were rich in proteins (Fig. 3a–c), whereas protease treated samples were rich in polysaccharides (Fig. 3d–f) relative to the control samples.

Fig. 4 shows the treatment effects of detergents and enzymes on the structural integrity, *i.e.*, HDD (size), zeta potential and PDI of Se, Te and Se–Te NPs, respectively. Overall, for protease treatment, the HDD significantly increased for all samples (Fig. 4a–c). The zeta potential significantly decreased for all the treatments, but more prominently in the protease treatment (Fig. 4d–f). Similarly, the PDI was markedly higher after Triton and protease treatment (Fig. 4g–i). All the three parameters revealed a hindrance in stability of the NPs, which can be correlated to particle aggregation as observed from the increasing HDD. The highly positive values of the zeta potential in the protease treated NP indicates the important role of proteins in maintaining the structural integrity of the NPs. The lowest value of the zeta potential and PDI, even after enzymatic (protease) degradation, in case of Se–Te NPs compared to the individual NPs indicates a better stability of the conjugated NP forms.

3.3. Characterization of NPs

Fig. 5 shows the FTIR spectra of the NPs in control and protease treated samples. The peak at 3200–3400 cm^{-1} correlates to the –

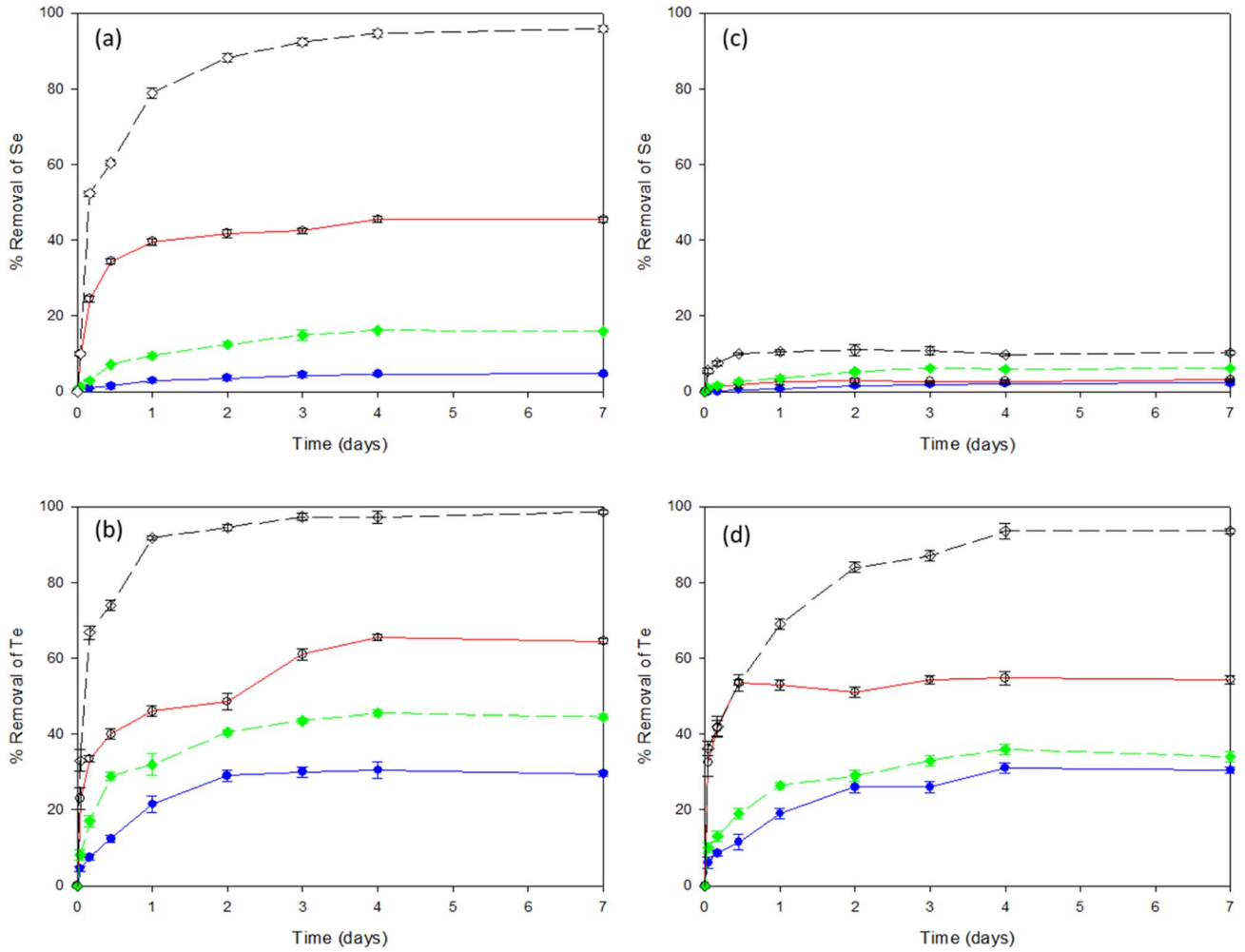

Fig. 1 Removal efficiencies of Se and Te oxyanions individually (a and b) as well as in combination (c and d) by LB-EPS, WAS (—●—), LB-EPS, AGS (—○—), TB-EPS, WAS (—◆—) and TB-EPS, AGS (—◇—), respectively.

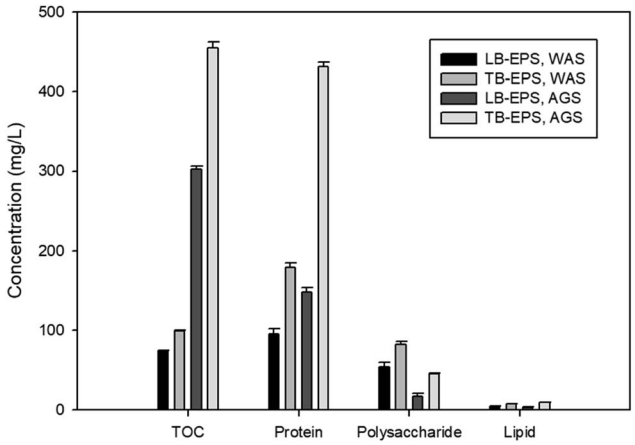

Fig. 2 Biochemical composition of LB and TB-EPS of WAS and AGS.

OH and –NH stretching vibrations of amine and carboxylic groups. The peaks at 2916 and 2848 cm^{-1} relate to the C–H stretching modes. The prominent peaks noticed at 1630 and 1546 cm^{-1} associate with the stretching vibration of C=O and N–H, respectively, in amide linkages of proteins. The band around 1462 cm^{-1} corresponds to an asymmetric vibrations of methyl or carboxylate groups. Another band observed between the range of 1070 and 1031 cm^{-1} represents C–H and C–O–C stretching from the carbohydrate groups. The spectra shows certain peaks at 1030, 1635, 2848 and 3400 cm^{-1} of the NP have shifted to 1035, 1627, 2800 and 3200 cm^{-1}, respectively, in protease treated samples. Thus, the shifting of these peaks indicates the interactions of mainly hydroxyl and carbonyl functional groups.

The TEM images revealed that the NPs produced from EPS were spherical in shape and were within 146–397 nm (Se NPs), 42.4–183 nm (Te NPs) and 24.7–123 nm (Se–Te NPs) in size (Fig. S2 in ESI†). The combined NPs of Se and Te were the smallest in size compared to the individual NPs.

The FEEM spectra of EPS extracted from the NPs are shown in Fig. 6. The major EPS components are a complex mixture of aromatic proteins, fulvic acid, humic substances and soluble microbial products. The change of intensities observed at excitation/emission wavelengths (Ex/Em) of 230/330, 280/330,

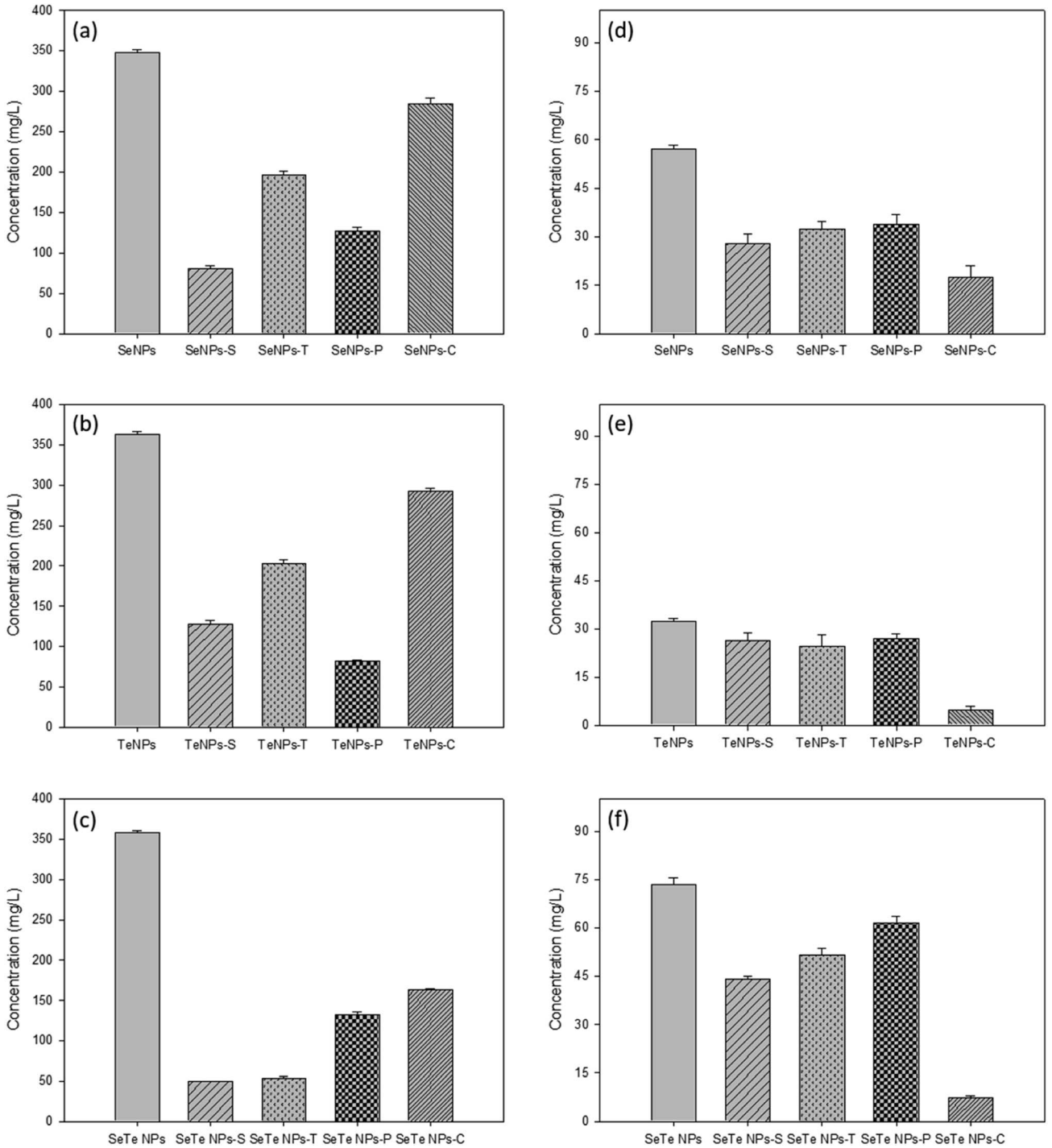

Fig. 3 Effect of various treatments (SDS: S, Triton: T, protease: P, cellulase: C) on protein (a–c) and polysaccharide (d–f) components of Se, Te and Se–Te NPs, respectively. The first bar represents the control sample in each plot.

and 312/380–420 nm, respectively, correspond to the soluble fraction of EPS. One main fluorescent peak was identified in the FEEM spectra of EPS samples of the control and the enzyme treated NPs. The main peak was identified at Ex/Em wavelengths of 260–290/310–350 nm which has been reported as a combination of protein-like substances and soluble microbial products. The fluorescence is mainly derived from the aromatic amino acid residues, *i.e.*, tyrosine and/or tryptophan. This is correlated with the quantitative results of EPS that showed the predominance of proteins in the NPs capping material.[9] The intensities corresponding to the aromatic proteins were similar in the control (Fig. 6a–c) and cellulase (Fig. 6g–i) treated samples, which were decreased in the protease treated samples (Fig. 6d–f).

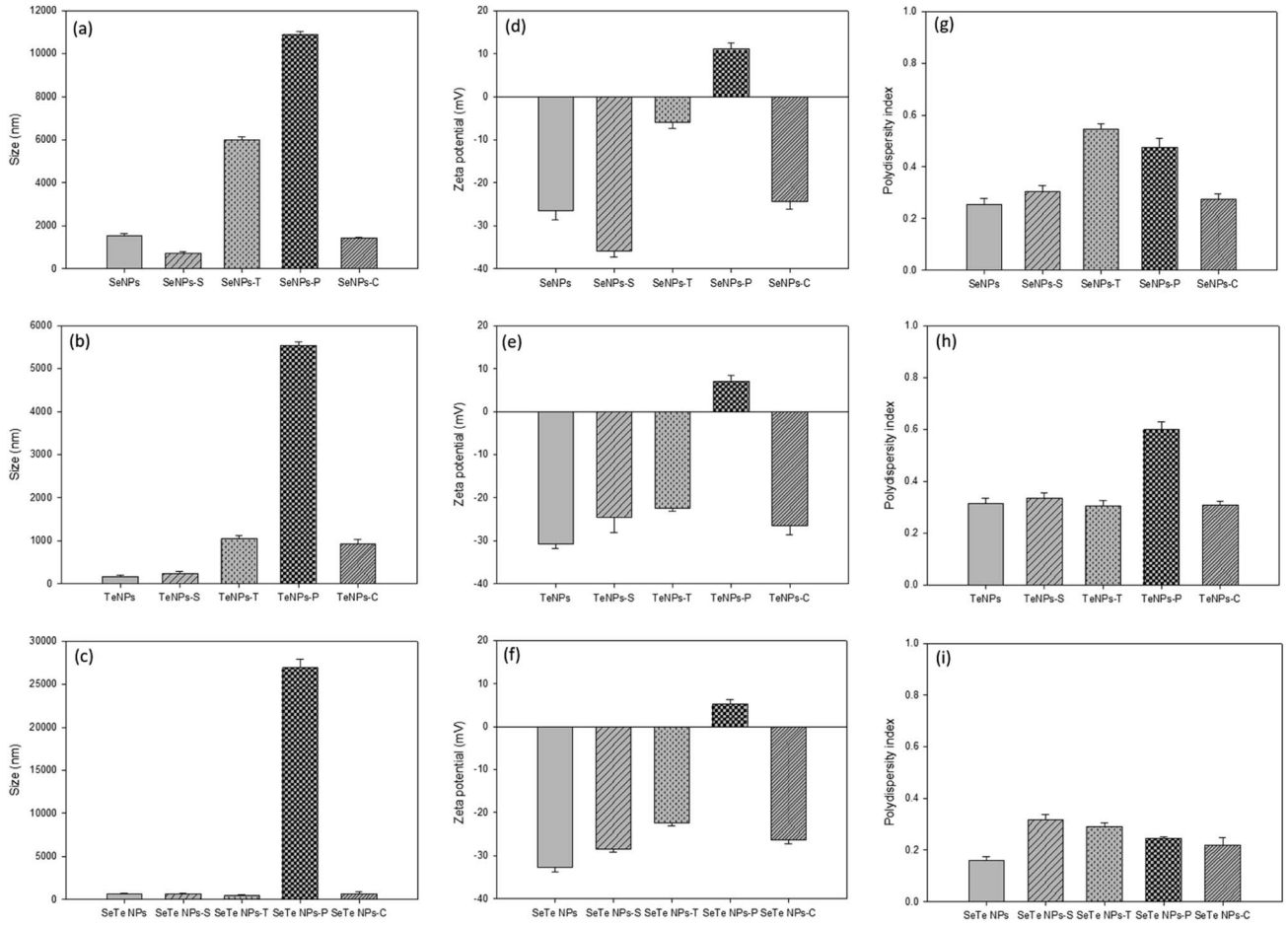

Fig. 4 Effect of various treatments (SDS-S, Triton-T, protease-P, cellulase-C) on size (a–c), zeta potential (d–f) and polydispersity index (g–i) of Se, Te and Se–Te NPs, respectively. The first bar represents the control sample in each plot.

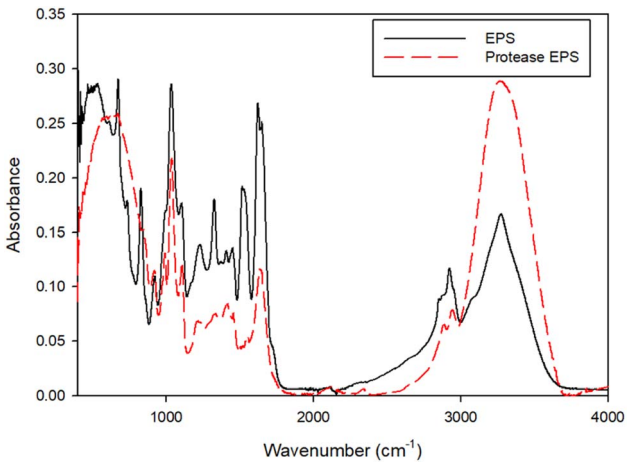

Fig. 5 FTIR spectra of EPS and protease treated EPS.

Fig. 7 shows the XRD patterns of Se, Te and Se–Te NPs, respectively. The XRD pattern of SeNPs showed main peaks at 2θ values of 26.93°, 27.5°, and 37.2°, corresponding respectively to the crystal planes (101), (102) and (111) for Se (Fig. 7a). The prominent peaks of TeNPs were observed at 2θ values of 23.5°, 27.7°, and 31.8°, corresponding to the (102), (110), (201) planes of hexagonal Te (Fig. 7b). Furthermore, the peaks at 27.7° and 29.3° confirm the presence of Se and Te NPs in Se–Te NPs (Fig. 7c). The different XRD pattern observed for the crystalline samples could be attributed to metastable state of the crystal.

Table 1 shows the DNA concentrations of the NPs in the control, protease and cellulase treated conditions. The amount of DNA was similar in the control and cellulase treated samples, whereas it was below the detection limit (>0.5 nanogram per millilitre) in protease treated samples. This signifies the presence of DNA in the EPS content of NPs, which might also be a contributing factor for their structural integrity in addition to the protein content.

4. Discussion

4.1. Reduction of selenite and tellurite by EPS

This study showed the reductive properties of EPS of anaerobic sludges in transforming selenite and tellurite oxyanions to their elemental nanoparticle forms (Fig. 1). The total TOC measurement (Fig. 2) indicated the amount of EPS extracted from the two different sludges investigated (waste activated sludge flocs and anaerobic sludge granules). EPS extracted from the

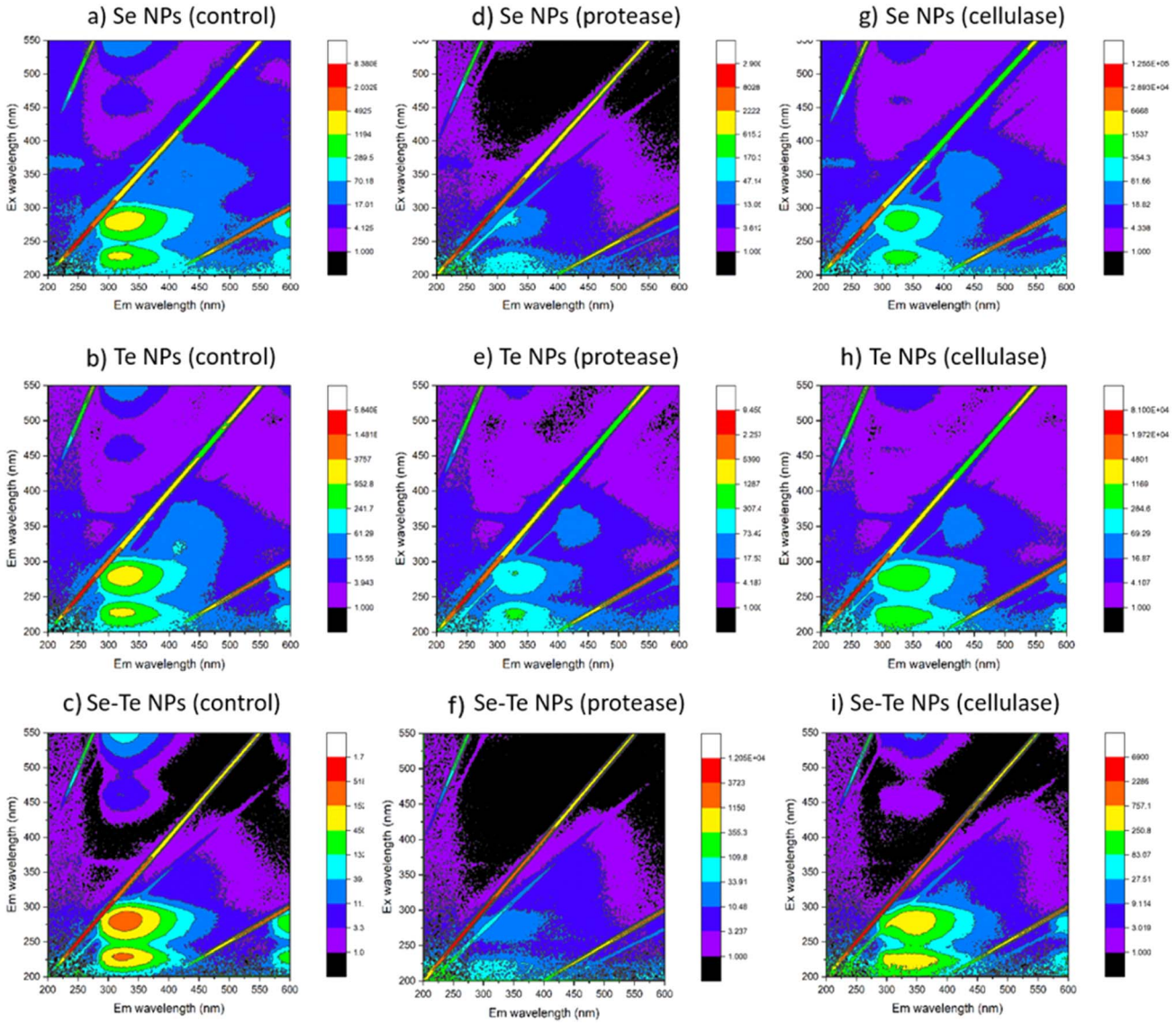

Fig. 6 FEEM spectra of control (a–c), protease (d–f) and cellulase (g–i) treated samples of Se, Te and Se–Te NPs.

granules contained less LB-EPS and more TB-EPS (Fig. 2), whereas WAS flocs possessed less TB-EPS and more LB-EPS. The higher removal of selenite and tellurite obtained by TB-EPS can also have contributed to the higher reduction efficiency of the AGS granules over the WAS flocs (Fig. 1). The presence of hydrophobic groups in the biochemical composition of EPS, majorly in the form of proteins (N–H groups) in TB-EPS, plays an important role in the stronger reduction efficiency than LB-EPS of both sludges as also reported for other anaerobic granular sludge types.[35] Quantitative analysis of the TB-EPS revealed proteins as the predominant component over polysaccharides and lipids as they are crucial for steric stabilization and destabilization of the cell surface.[36] The higher quantities of proteins in the TB-EPS of AGS granules and higher quantities of polysaccharides (Fig. 2 and 3) in the LB-EPS of WAS flocs also suggests the role of proteins in the reduction of selenite and tellurite. This correlates with the better core compaction and higher structural stability of granular sludge particles provided by TB-EPS[35] which could be attributed to better (>95%) removal efficiency. The role of EPS on the reduction of selenite to elemental selenium by activated sludge was reported by Zhang *et al.* (2020),[22] however, the specific fraction of EPS responsible for the reduction mechanism and the effect of granular sludge-EPS on selenite reduction were unknown.

The reducing activity is an important aspect of sludge EPS owing to the presence of several redox-active components.[22] Various functional groups of TB-EPS extracted from sludge granules were investigated owing to their highest reductive ability. The peaks of the FTIR spectra (Fig. 5) corresponding to the amides I and II as well as $-CH_2$ and aliphatic C–H, respectively, suggest the possible interactions of proteins in the reductive mechanism. The presence of thiol groups accordingly at the 2550 cm^{-1} peak suggest also thiol mediated reduction of selenite and tellurite. This is in concordance with the study of

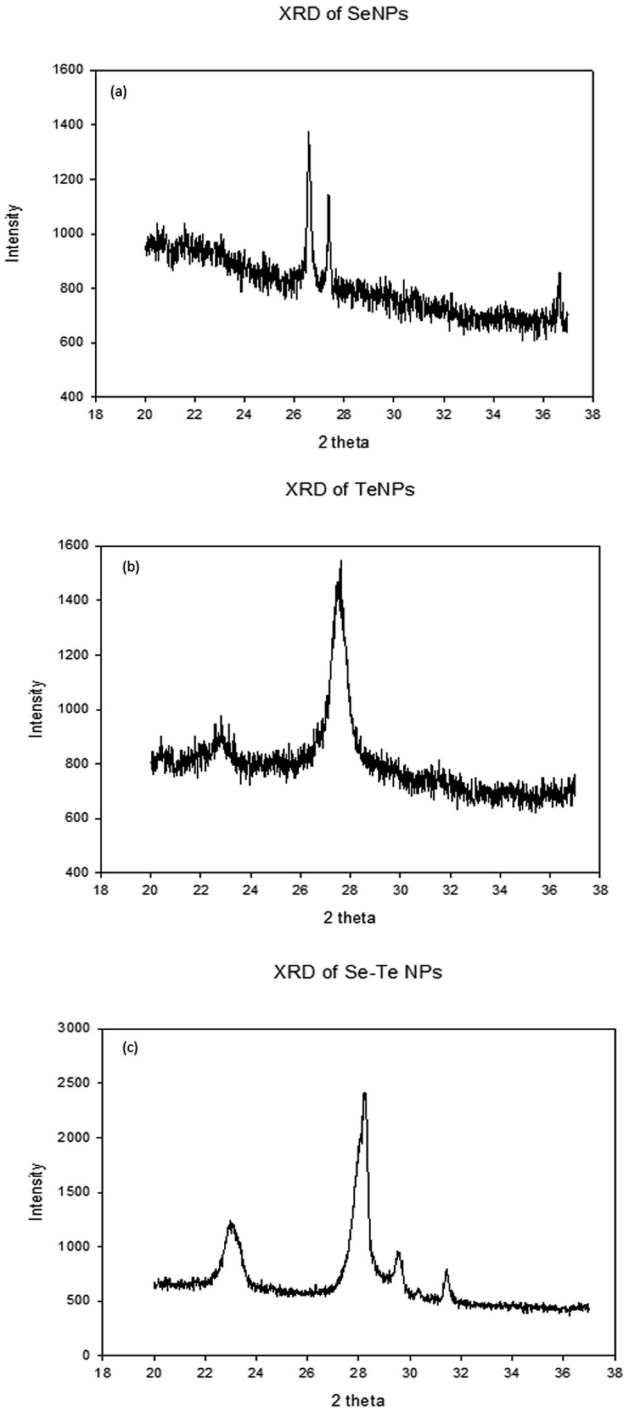

Fig. 7 XRD pattern of EPS-synthesized Se (a), Te (b) and Se–Te (c) NPs.

Table 1 Quantification of DNA (ng mL^{-1}) extracted from Se, Te and Se–Te NPs

Sample	Control	Protease treated	Cellulase treated
Se	15.2	Not detectable	14.0
Te	13	Not detectable	12.6
Se–Te	17.1	Not detectable	19.7

Gennari *et al.*,[37] where thiols first reduced the selenite to selenotrisulfides (–S–Se–S–), followed by the decomposition of –S–Se–S– to selenium in elemental forms. Moreover, the peak shifts at 1045 cm^{-1} and 1091 cm^{-1} as well as 985 cm^{-1} and 833 cm^{-1} for, respectively, selenite and tellurite before and after interaction with EPS correlates to the presence of polysaccharides. These changes in FTIR spectra suggest the interaction of reducing saccharides of EPS (mainly hemiacetal or aldehyde groups) which might also participate in the reduction of both chalcogen oxyanions as reported for selenite.[22]

The bands at 1259, 1082, and <1000 cm^{-1} correspond to the phosphate groups of nucleic acids.[38] Besides, the peak shift at 1236 cm^{-1} related to C–O stretching of phenols suggests that phenolic groups of EPS could also play a role in selenite and tellurite reduction.[22,39] The variation in composition of the organic fraction thus induces excellent binding abilities of the EPS. Overall, the presence of sulfhydryl proteins, extracellular enzymes (cytochromes and oxidoreductase) and reducing saccharides from the significant peaks present in the FTIR spectra can have contributed to TB-EPS mediated selenite and tellurite reduction.

4.2. Composition and structural stability of EPS mediated production of Se and Te NPs

Enzymatic treatments were more effective than the detergents to remove part of the capping material (Fig. 3). Triton mainly removed the proteins, whereas SDS removed a part of the polysaccharides in addition to proteins. Even though Triton removed less material compared to SDS treatment, the NPs' stability was less in Triton than in SDS in terms of the parameters HDD, PDI and zeta-potential. This could be due to the negatively charged dodecyl sulfate molecules of SDS that impart electrostatic repulsion between the particles and hence the NP stability. The critical micelle concentration (CMC) of SDS in water is reported to be 8.3 mM.[40] This implies that when the SDS concentration in water is below its CMC (0.35 mM, the concentration used in this study), the molecules are assumed to form a double-layer configuration.[41] In that case, the first layer of the SDS molecules containing hydrophilic head groups orient towards the inner particle surface, whereas the hydrophobic tails face outward. This leads to the formation of the second layer, where hydrophilic groups orient in an outward direction from the particle surface.[30] This double-layer coating structure generally enhances steric repulsion of SDS-coated NPs to retain their colloidal stability in aqueous solutions.[30]

On the other hand, a positive correlation was observed in case of enzymatic digestions between the component removed from the coating layer of NPs and their respective colloidal stability. The lower negative zeta potential and higher HDD and PDI values after protease treatment in all NPs indicated the destabilization of NPs without proteins (Fig. 4). The cellulase treated samples did not show any significant changes from the controls in terms of stability of the NPs. This was clearly evidenced from the FEEM spectra of the NPs (Fig. 6). The abundance of protein observed in the cellulase treated samples thus further implied the importance of protein-like substances of

EPS in stabilizing NPs as also reported in SeNPs and TiO_2 NPs.[31,32] Kusaka *et al.* (1976)[42] observed the presence of small globular protein in the extracellular protein fraction on the hydrophobic TiO_2 NPs surface that induces steric repulsive forces, thereby promoting the stability of the NPs. The importance of globular protein in stability has also been shown for single-walled carbon nanotubes (SWCNTs) and MnO_2 NPs.[31]

4.3. Effect of eDNA on NPs

Simultaneous removal of extracellular DNA (eDNA) in the protease treatment (Table 1) indicates their importance in structural integrity of NPs as indicated in Fig. 4. The destabilization of NPs after protease treatment could be interlinked with eDNA of the surface matrix as demonstrated in a previous study of eDNA and extracellular proteins including amyloid fibrils (AF) of EPS in protease treatment that suggests intermolecular linkages among the extracellular matrix components.[43] The majority of proteins as well as a small amount of nucleic acids (eDNA) and carbohydrates in microbial EPS are bridged by divalent ions, such as Ca^{2+} and Mg^{2+}.[44] The carboxyl groups of proteins become ionized under neutral conditions and are linked to the EPS matrix by such divalent metal ions.

eDNA may also be associated with the components present in the EPS matrix through physico-chemical interactions.[43] The structural assemblage of proteins and polysaccharides in the EPS matrix might hinder the extraction of eDNA from the matrix. This identifies the role of eDNA as a structural scaffold of EPS.[45] The aggregative mechanism of eDNA and protein has been investigated for bacterial biofilms where protease was found to be effective in biofilm destruction through weakening of the EPS matrix.[44] Thus, the simultaneous removal of protein (Fig. 4) and a fraction of eDNA (Table 1) after EPS removal treatments underline the role of these two components in the formation and structural stability of NPs in colloidal suspensions.

4.4. Characterisation of individual *versus* conjugated NPs

This study demonstrates that the composition and surface properties of Se and Te NPs alter when they are formed in conjugated form. The protease treatment indicated higher destabilization of Se–Te NPs than their individual form with higher HDD. Similarly, the removal of polysaccharides by cellulase did not show any significant changes in the composition of the individual NPs, except the conjugated forms (Fig. 3). This indicates the role of reducing polysaccharides along with proteins in maintaining the structural stability of the conjugated NPs. A small range of differences in the values of HDD (~100 μm) and zeta-potential (−31.5 to −33.5 mV) of the Te NPs and Se–Te NPs suggests the predominance of Te in Se–Te NPs, which could be further evidenced from the higher amount of tellurite reduction than selenite during co-synthesis. The higher negative zeta potential (~−8 mV) (Fig. 4f) and similar PDI values (0.25) (Fig. 4i) even after the enzymatic digestion place Se–Te NPs as more stable particles compared to their individual form in colloidal suspension. The negative surface charge of Se–Te NPs (Fig. 4f) can be attributed to a large number of carboxylic and amine groups as also seen for Se–S nanoparticles with an organic layer as a coating.[46]

Further characterization using TEM images shows the size of Se–Te NPs was smaller than those of their individual forms. The FEEM peaks (Fig. 6) located at the Ex/Em wavelengths of 220–230/340–370 nm and at the Ex/Em of 280/335–355 nm had more intensity than the individual NPs. Those two peaks were reported as protein-like substances of aromatic amino acid residues.[9] Therefore, the presence of more proteinaceous substances around the NPs coating (Fig. 3 and 4) might provide colloidal stability to NPs either by electrostatic or steric interactions. Moreover, the increase in HDD in the treated conditions, mainly in enzymatic digestion in the conjugated form (Fig. 4), is consistent with the results found from the FEEM spectra (Fig. 6). This could be further related to the higher negative zeta potentials of the Se–Te NPs (Fig. 4f). The presence of amino acids makes the surface of the NPs more hydrophobic, which enhances the steric repulsion thereby increasing the colloidal stability of NPs. In addition to the peaks of Se and Te, the secondary peaks observed in the XRD pattern at 2θ values of 29.5° and 31.3° of the conjugated forms might indicate phase conversion between Se–Te in crystal planes. Te/Se alloys composed of bound helical chains interact *via* van der Waals forces to form highly anisotropic crystal structures.[2] A further evaluation requires X-ray photoelectron spectroscopy (XPS) and extended X-ray absorption fine structure (EXAFS) analysis to understand the bonding interactions between the NPs and the EPS matrix.

4.5. Practical implication/future perspective

The present study revealed the previously unrecognized role of EPS in selenite and tellurite detoxification by microorganisms. These new findings complement the reductive detoxification mechanisms of microorganisms for hazardous selenite and tellurite. Given the ubiquity and abundance of microbial EPS in the environments, the uncovered role of EPS in selenite reduction implied that EPS can participate in the selenium–tellurium biogeochemical cycles and influence their speciation. Different environmental factors such as pH and dissolved oxygen should be further taken into consideration to evaluate the reduction efficiency of EPS in the natural environment. Besides, toxicity bioassays of the NPs are necessary for determining their potential adverse effects in natural environments.

The conjugated form of Se–Te NPs presented excellent surface properties compared to their individual forms (Fig. 4). The identification and regulation of the key components of the EPS are important for the structural stability of (conjugated) NPs, which might open up wider applications for engineered nanomaterials.

5. Conclusion

This work demonstrated that EPS from AGS and WAS reduce selenite to elemental selenium and tellurite to elemental tellurium nanoparticles efficiently in aquatic environments. The formed NPs as a result of reduction exhibited negative surface

charges of −22.8, −31.5 and −33.5 mV for Se, Te and Se–Te NPs, respectively. The thiols, reduced polysaccharides and phenolic groups of EPS were found to be the reducing groups for selenite reduction. Significant differences were found in individual and conjugated forms of Se–Te NPs. The higher surface charge (−33.5 mV), lower particle size (24.7–123 nm) and lower dispersity (0.2) infer more stable NPs in conjugated forms than in their individual form.

Ethical statement

This article is not associated with any studies with human participants or animals performed by any of the authors.

Author contributions

Sudeshna Saikia: conceptualization, investigation, formal analysis, data curation, visualization, writing – original draft. Kannan Pakshirajan: review & editing. Piet N. L. Lens: project administration, resources, supervision, funding acquisition, writing – review & editing.

Conflicts of interest

The authors declare that they have no conflict of interest.

Acknowledgements

This work was supported by the Science Foundation Ireland Research Professorship Innovative Energy Technologies for Biofuels, Bioenergy and a Sustainable Irish Bioeconomy (IETS-BIO^3; grant number 15/RP/2763) and the Research Infrastructure research grant Platform for Biofuel Analysis (Grant Number 16/RI/3401). The authors thank Borja Khatabi Soliman Tamayo, Leah Egan and Manuel Suarez (University of Galway, Ireland) for their help during the laboratory work. The authors acknowledge Olena Kudina and Oliver Carroll (Biomedical Engineering at University of Galway, Ireland) for assistance in zetasizer and Eadaoin Timmins (Centre for Microscopy and Imaging, University of Galway, Ireland) for TEM analysis.

References

1 E. Piacenza, A. Presentato, E. Zonaro, S. Lampis, G. Vallini and R. J. Turner, Microbial-based bioremediation of selenium and tellurium compounds, *Biosorption*, 2018, **4**, 1–8.

2 S. L. Wadgaonkar, J. Mal, Y. V. Nancharaiah, N. O. Maheshwari, G. Esposito and P. N. Lens, Formation of Se (0), Te (0), and Se (0) –Te (0) nanostructures during simultaneous bioreduction of selenite and tellurite in a UASB reactor, *Appl. Microbiol. Biotechnol.*, 2018, **102**, 2899–2911.

3 D. C. Vaigankar, S. K. Dubey, S. Y. Mujawar, A. D'Costa and S. K. Shyama, Tellurite biotransformation and detoxification by *Shewanella baltica* with simultaneous synthesis of tellurium nanorods exhibiting photo-catalytic and anti-biofilm activity, *Ecotoxicol. Environ. Saf.*, 2018, **165**, 516–526.

4 V. R. Kurimella, K. R. Kumar and P. D. Sanasi, A novel synthesis of tellurium nanoparticles using iron (II) as a reductant, *Int. J. Nanosci. Nanotechnol.*, 2013, **4**, 209–221.

5 Z. Li, Q. Sun, Y. Zhu, B. Tan, Z. P. Xu and S. X. Dou, Ultra-small fluorescent inorganic nanoparticles for bioimaging, *J. Mater. Chem. B*, 2014, **2**(19), 2793–2818.

6 Z. H. Lin, C. H. Lee, H. Y. Chang and H. T. Chang, Antibacterial activities of tellurium nanomaterials, *Chem.–Asian J.*, 2012, **7**(5), 930–940.

7 H. L. Seng and E. R. Tiekink, Anti-cancer potential of selenium-and tellurium-containing species: opportunities abound, *Appl. Organomet. Chem.*, 2012, **26**(12), 655–662.

8 Y. Bai, F. Rong, H. Wang, Y. Zhou, X. Xie and J. Teng, Removal of copper from aqueous solutions by adsorption on elemental selenium nanoparticles, *J. Chem. Eng. Data*, 2011, **56**(5), 2563–2568.

9 S. Saikia, A. Sinharoy and P. N. Lens, Adsorptive removal of gallium from aqueous solution onto biogenic elemental tellurium nanoparticles, *Sep. Purif. Technol.*, 2022, **286**, 120462.

10 M. C. Zambonino, E. M. Quizhpe, F. E. Jaramillo, A. Rahman, N. Santiago Vispo, C. Jeffryes and S. A. Dahoumane, Green synthesis of selenium and tellurium nanoparticles: current trends, biological properties and biomedical applications, *Int. J. Mol. Sci.*, 2021, **22**(3), 989.

11 Y. V. Nancharaiah and P. N. Lens, Ecology and biotechnology of selenium-respiring bacteria, *Microbiol. Mol. Biol. Rev.*, 2015, **79**(1), 61–80.

12 D. Song, X. Li, Y. Cheng, X. Xiao, Z. Lu, Y. Wang and F. Wang, Aerobic biogenesis of selenium nanoparticles by *Enterobacter cloacae* Z0206 as a consequence of fumarate reductase mediated selenite reduction, *Sci. Rep.*, 2017, **7**(1), 3239.

13 A. Sinharoy, S. Saikia and K. Pakshirajan, Biological removal of selenite from wastewater and recovery as selenium nanoparticles using inverse fluidized bed bioreactor, *J. Water Process. Eng.*, 2019, **32**, 100988.

14 S. M. Baesman, T. D. Bullen, J. Dewald, D. Zhang, S. Curran, F. S. Islam, T. J. Beveridge and R. S. Oremland, Formation of tellurium nanocrystals during anaerobic growth of bacteria that use Te oxyanions as respiratory electron acceptors, *Appl. Environ. Microbiol.*, 2007, **73**(7), 2135–2143.

15 E. Zonaro, E. Piacenza, A. Presentato, F. Monti, R. Dell'Anna, S. Lampis and G. Vallini, Ochrobactrum sp. MPV1 from a dump of roasted pyrites can be exploited as bacterial catalyst for the biogenesis of selenium and tellurium nanoparticles, *Microb. Cell Fact.*, 2017, **16**(1), 1–7.

16 S. M. Baesman, J. F. Stolz, T. R. Kulp and R. S. Oremland, Enrichment and isolation of *Bacillus beveridgei* sp. nov., a facultative anaerobic haloalkaliphile from Mono Lake, California, that respires oxyanions of tellurium, selenium, and arsenic, *Extremophiles*, 2009, **13**, 695–705.

17 X. Liang, M. A. Perez, K. C. Nwoko, P. Egbers, J. Feldmann, L. Csetenyi and G. M. Gadd, Fungal formation of selenium

and tellurium nanoparticles, *Appl. Microbiol. Biotechnol.*, 2019, **103**, 7241–7259.
18 P. V. Bhaskar and N. B. Bhosle, Microbial extracellular polymeric substances in marine biogeochemical processes, *Curr. Sci.*, 2005, **88**, 45–53.
19 H. C. Flemming and J. Wingender, The biofilm matrix, *Nat. Rev. Microbiol.*, 2010, **8**(9), 623–633.
20 W. W. Li and H. Q. Yu, Insight into the roles of microbial extracellular polymer substances in metal biosorption, *Bioresour. Technol.*, 2014, **160**, 15–23.
21 F. Kang and D. Zhu, Abiotic Reduction of 1,3-Dinitrobenzene by Aqueous Dissolved Extracellular Polymeric Substances Produced by Microorganisms, *J. Environ. Qual.*, 2013, **42**(5), 1441–1448.
22 X. Zhang, W. Y. Fan, M. C. Yao, C. W. Yang and G. P. Sheng, Redox state of microbial extracellular polymeric substances regulates reduction of selenite to elemental selenium accompanying with enhancing microbial detoxification in aquatic environments, *Water Res.*, 2020, **172**, 115538.
23 A. V. Tugarova and A. A. Kamnev, Proteins in microbial synthesis of selenium nanoparticles, *Talanta*, 2017, **174**, 539–547.
24 T. Tong, C. M. Wilke, J. Wu, C. T. Binh, J. J. Kelly, J. F. Gaillard and K. A. Gray, Combined toxicity of nano-ZnO and nano-TiO_2: from single-to multinanomaterial systems, *Environ. Sci. Technol.*, 2015, **49**(13), 8113–8123.
25 I. Jośko, P. Oleszczuk and E. Skwarek, Toxicity of combined mixtures of nanoparticles to plants, *J. Hazard. Mater.*, 2017, **331**, 200–209.
26 M. C. Zambonino, E. M. Quizhpe, F. E. Jaramillo, A. Rahman, N. Santiago Vispo, C. Jeffryes and S. A. Dahoumane, Green synthesis of selenium and tellurium nanoparticles: current trends, biological properties and biomedical applications, *Int. J. Mol. Sci.*, 2021, **22**(3), 989.
27 J. Mal, Y. V. Nancharaiah, I. Bourven, S. Simon, E. D. van Hullebusch, G. Guibaud and P. N. Lens, Cadmium selenide formation influences the production and characteristics of extracellular polymeric substances of anaerobic granular sludge, *Appl. Biochem. Biotechnol.*, 2021, **193**, 965–980.
28 J. Mal, Y. V. Nancharaiah, E. D. Van Hullebusch and P. N. Lens, Effect of heavy metal co-contaminants on selenite bioreduction by anaerobic granular sludge, *Bioresour. Technol.*, 2016, **206**, 1–8.
29 J. Mal, Y. V. Nancharaiah, N. Maheshwari, E. D. van Hullebusch and P. N. Lens, Continuous removal and recovery of tellurium in an upflow anaerobic granular sludge bed reactor, *J. Hazard. Mater.*, 2017, **327**, 79–88.
30 A. Bulgarini, S. Lampis, R. J. Turner and G. Vallini, Biomolecular composition of capping layer and stability of biogenic selenium nanoparticles synthesized by five bacterial species, *Microb. Biotechnol.*, 2021, **14**(1), 198–212.
31 D. Lin, S. D. Story, S. L. Walker, Q. Huang and P. Cai, Influence of extracellular polymeric substances on the aggregation kinetics of TiO_2 nanoparticles, *Water Res.*, 2016, **104**, 381–388.
32 Z. Lili, J. Liying, F. Fang and C. Jianmeng, Extraction and composition analysis of EPS for aerobic granular sludge, *Chin. J. Environ. Eng.*, 2007, **1**(4), 127–130.
33 R. Jain, N. Jordan, S. Weiss, H. Foerstendorf, K. Heim, R. Kacker, R. Hübner, H. Kramer, E. D. van Hullebusch, F. Farges and P. N. Lens, Extracellular polymeric substances govern the surface charge of biogenic elemental selenium nanoparticles, *Environ. Sci. Technol.*, 2015, **49**(3), 1713–1720.
34 L. Neves, M. A. Pereira, M. Mota and M. M. Alves, Detection and quantification of long chain fatty acids in liquid and solid samples and its relevance to understand anaerobic digestion of lipids, *Bioresour. Technol.*, 2009, **100**(1), 91–96.
35 L. Zhu, J. Zhou, M. Lv, H. Yu, H. Zhao and X. Xu, Specific component comparison of extracellular polymeric substances (EPS) in flocs and granular sludge using EEM and SDS-PAGE, *Chemosphere*, 2015, **121**, 26–32.
36 X. Y. Li and S. F. Yang, Influence of loosely bound extracellular polymeric substances (EPS) on the flocculation, sedimentation and dewaterability of activated sludge, *Water Res.*, 2007, **41**(5), 1022–1030.
37 F. Gennari, V. K. Sharma, M. Pettine, L. Campanella and F. J. Millero, Reduction of selenite by cysteine in ionic media, *Geochim. Cosmochim. Acta*, 2014, **124**, 98–108.
38 K. E. Eboigbodin and C. A. Biggs, Characterization of the extracellular polymeric substances produced by *Escherichia coli* using infrared spectroscopic, proteomic, and aggregation studies, *Biomacromolecules*, 2008, **9**(2), 686–695.
39 H. A. Abdulla, E. C. Minor, R. F. Dias and P. G. Hatcher, Changes in the compound classes of dissolved organic matter along an estuarine transect: a study using FTIR and 13C NMR, *Geochim. Cosmochim. Acta*, 2010, **74**(13), 3815–3838.
40 D. R. Perinelli, M. Cespi, N. Lorusso, G. F. Palmieri, G. Bonacucina and P. Blasi, Surfactant self-assembling and critical micelle concentration: one approach fits all?, *Langmuir*, 2020, **36**(21), 5745–5753.
41 A. Wołowicz and K. Staszak, Study of surface properties of aqueous solutions of sodium dodecyl sulfate in the presence of hydrochloric acid and heavy metal ions, *J. Mol. Liq.*, 2020, **299**, 112170.
42 I. Kusaka, K. Hayakawa, K. Kanai and S. Fukui, Isolation and Characterization of Hydrophobic Proteins (H Proteins) in the Membrane Fraction of *Bacillus subtilis*: Involvement in Membrane Biosynthesis and the Formation of Biochemically Active Membrane Vesicles by Combining H Proteins with Lipid, *Eur. J. Biochem.*, 1976, **71**(2), 451–458.
43 I. Randrianjatovo-Gbalou, P. Rouquette, D. Lefebvre, E. Girbal-Neuhauser and C. E. Marcato-Romain, *In situ* analysis of *Bacillus licheniformis* biofilms: amyloid-like polymers and eDNA are involved in the adherence and aggregation of the extracellular matrix, *J. Appl. Microbiol.*, 2017, **122**(5), 1262–1274.
44 O. Mitrofanova, A. Mardanova, V. Evtugyn, L. Bogomolnaya and M. Sharipova, Effects of *Bacillus* serine proteases on the bacterial biofilms, *BioMed Res. Int.*, 2017, **2017**, 8525912.

45 D. W. Hiebner, C. Barros, L. Quinn, S. Vitale and E. Casey, Surface functionalization-dependent localization and affinity of SiO_2 nanoparticles within the biofilm EPS matrix, *Biofilm*, 2020, **2**, 100029.

46 M. Vogel, S. Fischer, A. Maffert, R. Hübner, A. C. Scheinost, C. Franzen and R. Steudtner, Biotransformation and detoxification of selenite by microbial biogenesis of selenium-sulfur nanoparticles, *J. Hazard. Mater.*, 2018, **344**, 749–757.